IRAN: laboratory test bench for hypertelescope pupil-plane recombination

F. Allouche[a,b], F. Vakili[b], A. Glindemann[a], E. Aristidi[b], L. Abe[b], E. Fossat[b], R. Douet[b]

[a]ESO, Karl-Schwarzschild-strasse 2, 85748, Garching bei München, Germany;
[b]Laboratoire H. Fizeau, Université de Nice Sophia-Antipolis, CNRS UMR 6525 Parc Valrose, 06108 Nice Cedex 2, France

ABSTRACT

In 2004, our group proposed IRAN, an alternative beam-combination technique to the so-called hypertelescope imaging method introduced by Labeyrie in the 1990s. We have recently set up a laboratory experiment aiming at validating our image densification approach instead of the pupil densification scheme of Labeyrie. In our experiment, seven sub-apertures illuminated by laser sources are recombined using the IRAN scheme. The validation of the IRAN recombination consists basically in retrieving the point-spread intensity distribution (PSID), demonstrating the conservation of the object-image convolution relation. We will introduce IRAN, compare it to the hyper-telescope, and present the experimental results that we obtained.

Keywords: High angular resolution, Optical Interferometry, Imaging, Beam-combination

1. INTRODUCTION

In the permanent race towards always better and always more, astronomers have already thought about the next generation optical interferometers that will presumably be developed at the kilometric scale and beyond. Today the VLTI, with maximum baseline of 130 meters for the UTs and 200 meters for the AT's, is already providing us with visibility curves. Tomorrow, giant interferometric arrays (huge baseline and few tens of apertures), will enable us the access to sharp and high angular resolution images of celestial objects. Indeed, it has been proven that interferometers can be exploited in direct imaging mode thanks to Labeyrie's densified hypertelescope technique.[1]

In this ambitious context, Vakili *et. al* proposed a 39-telescope array, Kiloparsec Explorer for Optical Exoplanet Search, KEOPS,[6] to be built at Dome C of Antarctica. KEOPS is a deployable array of three concentric rings with 7, 13, 19 1.5 m telescopes. The primary goal of KEOPS is the direct detection and the spectral characterization of exoplanets (ExPNs), ultimately hunting exo-Earths in habitable zones. This is done following the nulling method called IRAN.[2]

Despite its pioneering position in the exploitation of interferometers in the imaging mode, in Labeyrie's technique[1] the objet-image convolution relation is modified by the intensity being modulated by the Airy envelope in the image plane. So instead of reconfiguring the pupils, Vakili[2] suggested reconfiguring the images through a concept presented in 2004 under the name of IRAN (Interferometric Remapped Array Nulling). In this paper, we will recall the IRAN concept with its main features, most importantly the recovery of the objet-image convolution relation over a field limited to the super-imposed pupil of the primary telescopes, called hereafter the metapupil. We will present afterwards the laboratory experiment set for the validation of this recombination concept. And we will discuss by the end of the paper the first results obtained.

2. PRINCIPLE OF IRAN

The method of beam combination that we propose is an alternative to the densified hypertelescope[1] technique introduced by Labeyrie in optical interferometry. The concept of the latter, as its name indicates, is to densify the pupil without introducing any geometrical changes to the array. The densification can be achieved either by
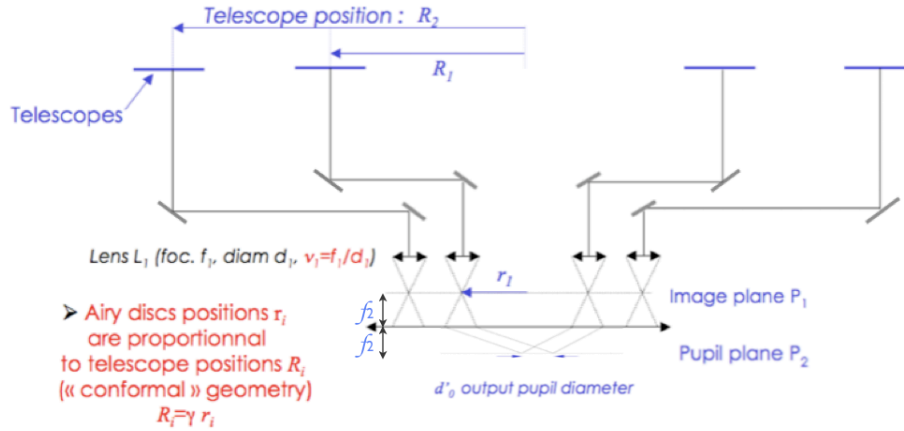
FIG. 1. The 1D IRAN set up scheme illustrated in this figure is fidele to the "conformal" geometry presented by Labeyrie as the condition for obtaining high-angular resolution images using interferometers. An array of L_i lenses, all identical in diameter and focal length, form in their common image plan P_1 the individual images given by each aperture. We thus obtain an array of Airy patterns where the position r_i of every single Airy pattern is set proportional to the position R_i of the corresponding telescope in order to remain "conformal". The Airy patterns are then recombined using a relay lens. In the focal plane of the latter, or the pupil plane, here denoted by P_2, we obtain a fringed pupil image.
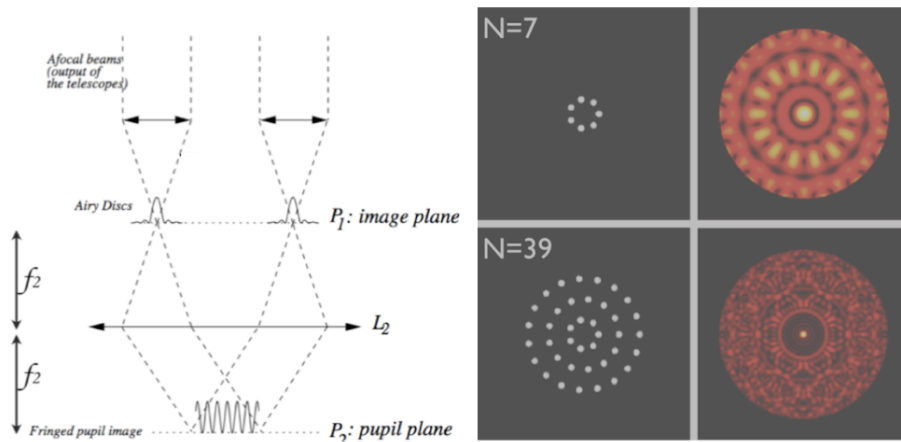

FIG. 2. This figure presents the fringed pupil image for an N-aperture interferometer. The left part of the figure represents a 1D scheme of the IRAN recombination in the very simple case of only 2 apertures. The right part of the figure represents a 2D scheme for N input pupils and their corresponding intensity in the pupil plane for an on-axis source. The $N = 39$ configuration is the entire scheme of the KEOPS antarctic interferometer, whereas the $N = 7$ configuration is a subset of KEOPS, the first ring of its diluted pupil. The fringed image tends more and more towards a pseudo-Airy function when N increases.

increasing the relative size of the elementary apertures or by gathering them to fill up the disk of an equivalent single dish. This, for instance, can be done by reimaging the output pupil using a pyramidal beam combiner.[7] Thus, the diffraction pattern of a hypertelescope, when all sub-apertures are cophased, resembles the one of a monolithic giant dish. In the IRAN beam-recombination concept, illustrated in Fig. 1, it is the elementary images, given by each telescope, that are reconfigured using a modified Michelson Periscopic[4] set up (or a pyramidal beam combiner depending on the scheme). A relay lens is then used to combine the sub-images leading to a diffraction pattern that, on one hand, is the equivalent to the one of a single giant dish and, on the other hand, conserves the object-image convolution relation.

2.1 The intensity distribution of off-axis sources

In this section we will recall the analytical expressions of the intensity in both image and pupil planes[2] (resp. P_1 and P_2) for off-axis sources and monochromatic light. The definitions of the parameters are :
  – N : the total number of aperture in the interferometric array each located at R_i
  – λ : the wavelength
  – d_1 and f_1 : the diameter and the focal length of each single lens
  – L_2 symbolizes the recombining or relay lens whose focal length is denoted f_2.

2.1.1 Off-axis Point source

When observing, at a given wavelength λ, an off-axis source in the direction $\boldsymbol{\theta}$ the image at the focus of every telescope will be shifted. This shift will lead to a piston term p_i that is a function of every single telescope's position R_i :

$$p_i = \exp\frac{2i\pi\boldsymbol{\theta}\mathbf{R_i}}{\lambda}, \tag{1}$$

therefore the complex amplitude in the image plane P_1 is given by :

$$\psi_1(\boldsymbol{\rho}) = A(\boldsymbol{\rho}) * \sum_{i=1}^{N} p_i \delta(\boldsymbol{\rho} - \boldsymbol{\rho}_i), \tag{2}$$

where $\boldsymbol{\rho}$ is the position vector in the image plane P_1, $\delta()$ the Delta Dirac distribution and finally A is the amplitude distribution given by the lenses for each afocal beam. For circular aperture $|A(\boldsymbol{\rho})|^2$ is an Airy disk of diameter $2.44\lambda f_1/d_1$. The intensity distribution in the plane P_1 is the square modulus of $\psi_1(\boldsymbol{\rho})$. It is the superposition of N Airy disks distributed with the same geometry than the diluted input pupil.

L_2 gives in the pupil plane P_2 the Fourier Transform of ψ_1 and on a 2D detector we can record its corresponding intensity, or PSID for point-spread intensity distribution :

$$I_2(\mathbf{r}) = |P(\mathbf{r})|^2 . \left| \sum_{i=1}^{N} \exp\left(-\frac{2i\pi(\mathbf{r} - \gamma f_2\boldsymbol{\theta}).\boldsymbol{\rho}_i}{\lambda f_2} \right) \right|^2, \tag{3}$$

where $\mathbf{r}$ is the position vector in the plane P_2, $\gamma = \mathbf{R_i}/\mathbf{r_i}$ is the densification factor. And in Eq. 3 $P(\mathbf{r})$ is the Fourier transform of $A(\boldsymbol{\rho})$. And its square modulus in Eq. 3 is the achromatic pupil function. In the ideal case of a circular aperture, the latter is a uniform disk of diameter $d_1 f_2/f_1$. It is straightforward to see that this function constitutes the physical limit of the field of view. The square modulus of the sum of the exponential term is the interference function that we shall denote from now on I_0. With $I_0(\mathbf{r}) = \left| \sum_{i=1}^{N} \exp\left(-\frac{2i\pi\mathbf{r}.\boldsymbol{\rho}_i}{\lambda f_2} \right) \right|^2$.

2.1.2 Off-axis Extended source

Considering an extended source with a brightness distribution $O(\boldsymbol{\theta})$, the final intensity in P_2 becomes[5] :

$$I_2(\mathbf{r}) = \frac{1}{(\gamma f_2)^2} |P(\mathbf{r})|^2 \left[I_0(\mathbf{r}) * O\left(\frac{\mathbf{r}}{\gamma f_2} \right) \right]. \tag{4}$$

Eq. 4 shows us how the objet-image convolution relation has been retrieved inside the limits set by the pupil function. The convolution relation is scaled by a factor γf_2 that allows us to convert a position x (meters) in the focal plane into radian angles on the sky $\boldsymbol{\theta} = x/(\gamma f_2)$.
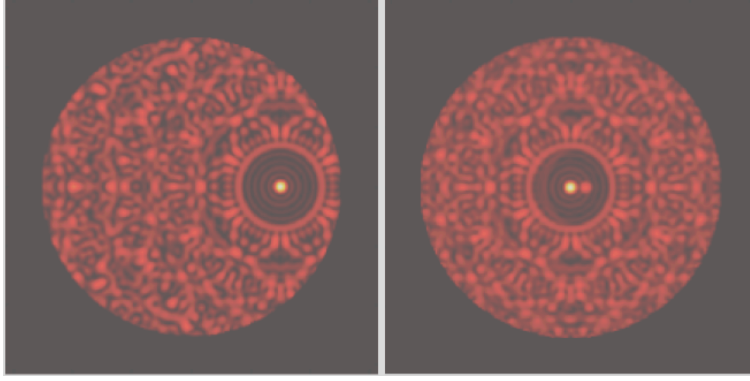
FIG. 3. Numerical simulations for an off-axis source at $\theta = 0.3$" (left) and for a binary (right) where the angular separation is 50 mas and a magnitude difference of 3. The FOV is 500 mas and the interferometer resolution is 30 mas. The PSID formed by the fringes shifts inside the envelope (geometric output pupil) without deformation and extinction (translation invariance). The envelope does not move. That is the main difference[3] with the Michelson/Labeyrie densified pupil setup.

3. THE LABORATORY EXPERIMENT

We describe here a laboratory optical prototype designed to confirm the optical properties of the IRAN scheme, e.g.
– studying the on-axis monochromatic PSID properties
– testing the translation invariance for an off-axis source and the object-image pseudo convolution relation
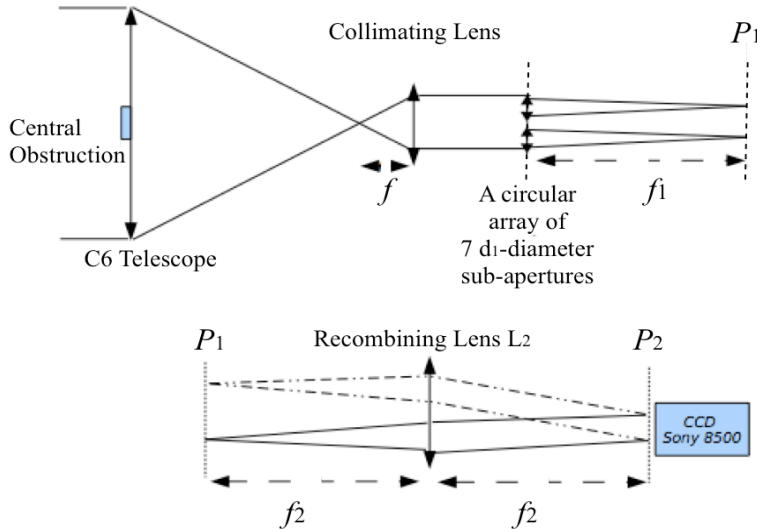– in a further step studying the polychromatic case

FIG. 4. Optical scheme of the science part of the experimental test bench.

The optical design is presented in Fig. 4. An incident plane wave is sent through an afocal beam compressor. In the output pupil plane, a mask with 7 holes holding 7 mini lenses simulates the afocal beams coming from the telescopes of a 7-aperture interferometer. The remainder of the optical bench is composed of a recombining lens and a CCD camera at its focus.

For a sake of simplicity, we chose not to use a periscopic setup for densifying the images such as in Fig. 1. The present design is indeed intrinsically cophased and allows quick access to the interferometric PSID. This simplicity would also allow to place the instrument onto an equatorial mount and observe the sky.

3.1 The Experimental Scheme

In this section we will present the optical components of the bench along with their characteristics.

3.1.1 The "source" part

The light source is a Ne-Ne laser ($\lambda = 632.8$ nm) followed by a microscope objective which feeds a 10 μm diameter pinhole (see Fig. 5). The diffracted beam is collimated by a so-called "C6" telescope (diameter 15 cm, focal ratio $f/d = 10$). The pinhole diameter is roughly the size of the Airy disk of the telescope. The ensemble laser+microscope objective+pinhole can be translated in the direction perpendicular to the optical axis, in order to provide an off-axis point-source. The characteristics of the C6 telescope are illustrated in Fig. 6.
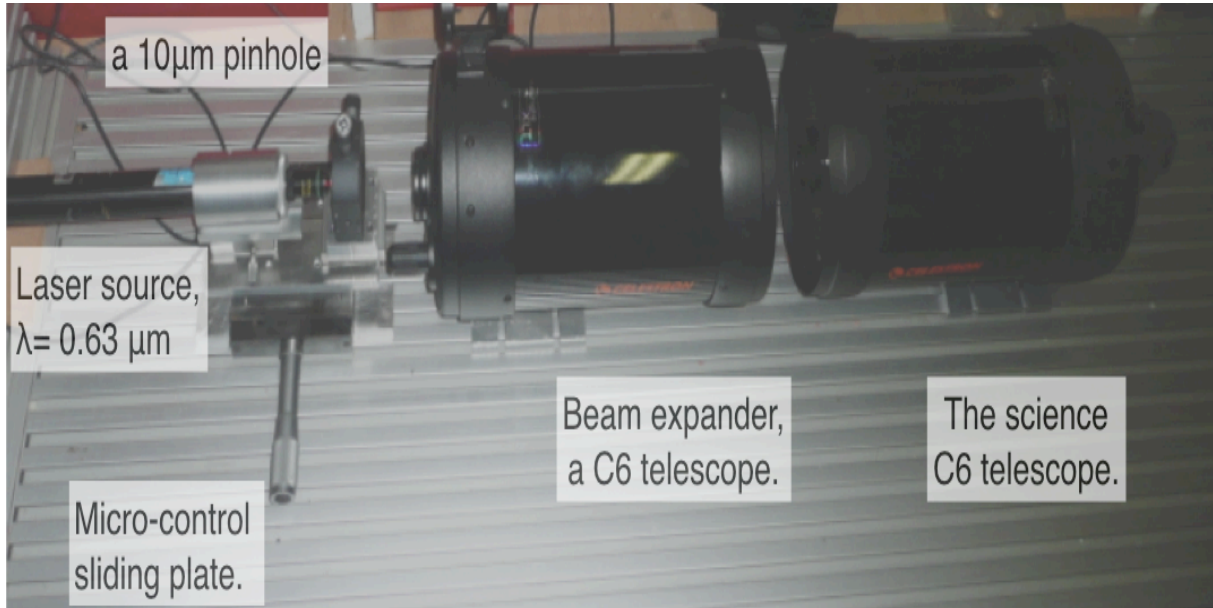

FIG. 5. A photo of the experiment. It shows the "source" part of the bench (laser+pinhole+beam expander) and the "science" telescope (also a C6) which collects the incident light.
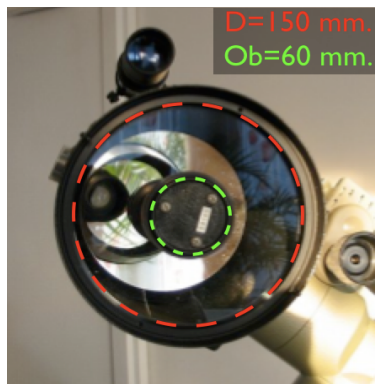

FIG. 6. Pupil entrance of the C6 telescope. Its diameter is equal to 150 mm. The telescope features a central obstruction whose diameter is 60 mm. The focal length is 1.5 m.

3.1.2 The "science" part

The science part, displayed is Fig. 7, starts with the second C6 telescope. Its input pupil contains the 7 sub-apertures of the interferometer. Our first idea was to place a 7 holes mask at its entrance, but it appeared to be unnecessary as we will see hereafter. This C6 is the first element of an afocal beam compressor, a collimating lens of diameter 19 mm and focal length 90 mm being the second one. The parallel light beam is compressed by a factor 17 and has a diameter of 9 mm with a central obstruction of 3.6 mm.

The beam is intercepted by an opaque mask containing a ring of seven circular sub-apertures (Fig. 8). Each sub-aperture has a diameter $d_1 = 1.9$ mm, the diameter of the ring is 6 mm. The output collimated beam is spatially filtered through these sub-apertures : this is the reason why we did not place any mask in the entrance pupil of the telescope.

Each sub-aperture contains a small lens of focal length of 193 mm. These $f/100$ lenses were specially manu-factured for the needs of our experiment. In the common focal plane of the lenses, the image plane P_1, we thus obtain 7 adjacent Airy patterns which are distributed over a 6 mm diameter circle. Each Airy disk size has a diameter of 150 μm.

The last optical element is a recombination lens L_2 (diameter 25 mm and focal 350 mm) which forms the interferometric image at its focus (P_2 plane). The fringe size is 37 μm. We record the PSID on a CCD camera (SONY PROGRESSIVE 8500CE) having a matrix of 782x582 pixel. The pixel size is 8.3 μm. We have a com-fortable sampling of 4 pixels per fringe.
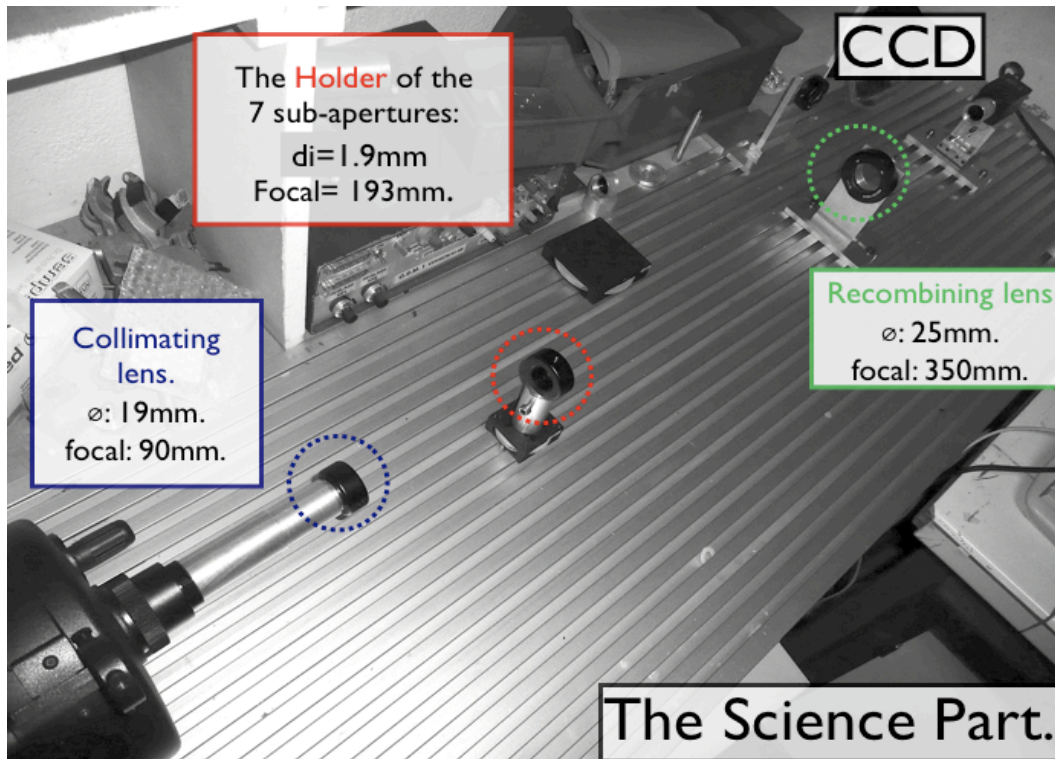

FIG. 7. The Science part of the test bench.

4. TESTING THE MINI-LENSES

The perhaps most challenging and time consuming part of the experiment is related to the mini-lenses, from their acquirement to their insertion in the test bench. Each lenslet has a diameter of 2 mm and a focal ration f/100. This is quite uncommon, and they were specially designed and manufactured by Sud-Est Optique de Précision, France. About 50 mini-lenses were realised in the perspective of a more sophisticated experiment.

The mechanical device that holds them together (Fig. 8) is a sandwich of three layers of aluminium disks 2.54 cm diameter. The first and third layer feature 7 1.9 mm diameter holes, uniformly distributed over a 6 mm diameter circle. The second layer is the same as the two described previously except that each hole has a diameter of 2.1 mm (instead of 1.9). The lenses are inserted in this intermediate layer. The ensemble is then placed in a standard lens holder.

FIG. 8. Mechanical support of the mini-lenses.

Our first task, before we could work properly with the interferometric bench, was to qualify the mini-lenses. These lenses are indeed prototypes and likely to suffer from various optical aberrations. We then realised a test bench (Fig. 9) in which the lenses are placed onto a transparent microscope parallel glass plate and illuminated by a collimated 35 mm diameter laser beam. The glass plate can hold up to 5 lenses. In the focal plane (see Fig. 10), we observe the Airy disk of the lens, as well as its geometrical shadow. The center of this shadow gives the position of the optical axis.
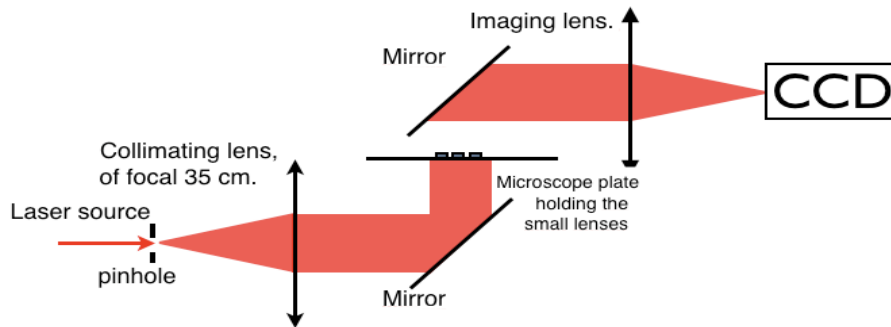

FIG. 9. This is the design of the set up for testing the lenses. As seen from the side i.e the microscope plate holding the lenses, and the 45° titled mirrors are parallel to the test bench.

The selection identifies three main features for each lens :
– the shape of the Airy pattern
– the displacement of the center of the Airy pattern with respect to the center of the optical axis of the lens (tilt introduced on the wavefront by the lens)
– The defocus
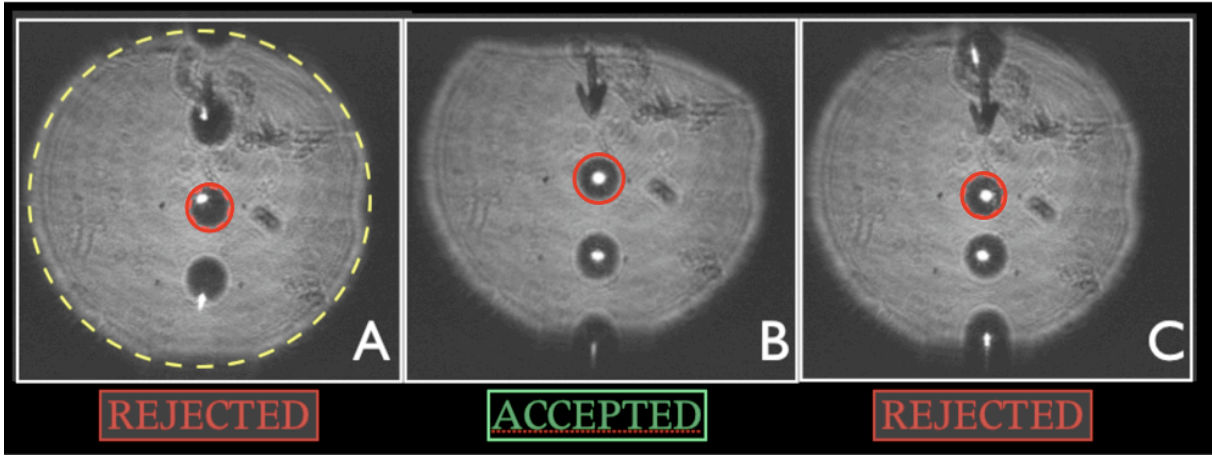We selected the 7 best lenses for the IRAN bench.

FIG. 10. Sample of images of the diffraction pattern given by the mini-lenses during the test. The large circle is the image of the beam. The small circle at the center is the relevant image of the lens under test. The small intense spot in the middle is the Airy pattern. Here we have presented 3 cases, both images A and C show clearly a tilt effect of the lens as can be concluded from the de-centered Airy disk. The position of the Airy pattern is almost at the edge of the geometrical image of the lens in image A and is not centered well enough in the geometrical image of the lens in image C. Image B is the good case.

5. THE FIRST RESULTS

The first experimental results will be divided in two parts. The results obtained in the image plane P_1. And the PSID images obtained on the CCD in the pupil plane P_2. Indeed, the characteristics of the images of the image plane and their quality are related to the quality of the beam, the optics as well as the bench alignment itself. In the image plane P_1, and despite all the care we have put in choosing the lenses, even the best one of them still exhibit a slight small tilt effect (see Fig. 11). We are expecting these small optical aberrations, that do not seem to be leading to catastrophic results in the image plane, to completely distort the PSID. Indeed, the PSID, leaving apart the achromatic function pupil developed in equation 3, is basically an interfering image. And the latter, in the optical range is very delicate and is busted as soon as we have small phase shifts or different optical paths between the different combined beams.
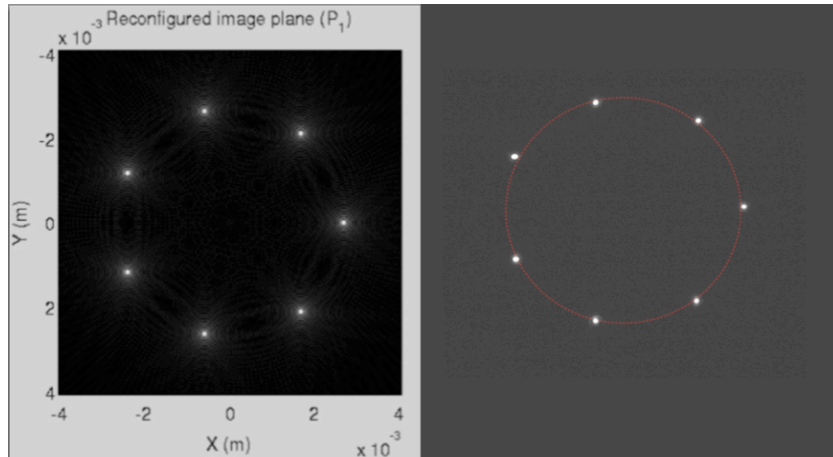

FIG. 11. Theory versus Experiment : Intensity distribution in P_1. The left plot represents numerical simulations obtained for the same optical characteristics of our bench. The right plot on the other hand is the experimental image. Both images are very similar. The Airy pattern in the experimental one are almost co-centric.
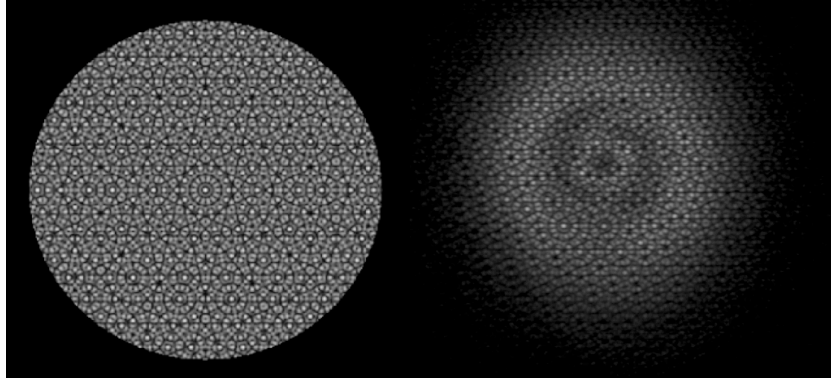
FIG. 12. Theory versus Experiment : Intensity in the pupil plane. The left plot is a numerical simulation of the PSID we are supposed to obtain with our test bench. The experimental image (right) of the pupil plane was obtained using the test bench as described in Fig. 4. As a matter of fact the image was taken right after doing the lenses' selection test, the test bench was then free of C6 telescopes (see Fig. 9). Thus the PSID seems to be multiplied by an nonhomogeneous diffraction pattern that is the result of an uncontrolled, or well calibrated, propagation of the light (absence of the telescopes) on one hand and definitely a poor precision in the placement of the different optics in the exact planes. The tiny peak at the center of the PSID, representing the image of a point is still missing in the experimental result due to the problems noted above.

6. CONCLUSION & DISCUSSION

Although the experiment is still young, the first results seem promising. The image of the image plane is rather reassuring since it is the key of obtaining good quality interferences images. Despite the poor quality of the pupil plane, we do believe that reinserting the telescopes will produce a much better fringed pupil image. And if this is true (still to be seen) then we are close to achieving one goal the test bench was designed for. However we are far from being done. We still have to validate the object-image convolution relation as an immediate second step. We would also like to image different sources, extended, polychromatic in order to test the robustness of the IRAN beam recombination concept.

REFERENCES

[1] Labeyrie A., 1996, A&A Suppl. 118, 517.

[2] Vakili F., Aristidi E., Abe L. and Lopez B., 2004 A&A, 421, 174

[3] Abe L., 2004, Proc, SPIE. Volume 5491 : *New Frontiers in Stellar Interferometry*, p.1519-1527.

[4] Michelson A. A., 1920, ApJ 51, 257.

[5] Goodman J.W., 1996, Introduction to Fourier Optics, Mc Graw-Hill Science.

[6] Vakili F. *al.*, 2004, Proc, SPIE. Volume 5491 : *New Frontiers in Stellar Interferometry*, p.1580-1586.

[7] Gillet, S., Riaud, P., Lardière O., Dejonghe J., Schmitt J., Arnold L., Boccaletti A., Horville D., Labeyrie, A., 2003, A&A 400, 393